Speed Control of Interior Permanent Magnet Synchronous Motor Drive for Flux Weakening Operation

Jang-Mok Kim, Seung-Ki Sul

School of Electrical Engineering, Seoul National University,

Sillim-Dong, Kwanak-Ku, Seoul, Korea.

Abstract - **A novel flux-weakening scheme for an Interior Permanent Magnet Synchronous Motor (IPMSM) is proposed. It is implemented based on the output of the synchronous PI current regulator - reference voltage to PWM inverter. The on-set of flux weakening and the level of the flux are adjusted inherently by the outer voltage regulation loop to prevent the saturation of the current regulator. Attractive features of this flux weakening scheme include no dependency on the machine parameters, the guarantee of current regulation at any operating condition, and smooth and fast transition into and out of the flux weakening mode. Experimental results at various operating conditions including the case of detuned parameters are presented to verify the feasibility of the proposed control scheme.**

I. INTRODUCTION

Interior permanent magnet synchronous motor (IPMSM) has gained the increasing popularity in recent years for various industrial drive applications. Magnets are buried inside the rotor core with a steel pole piece in the IPMSM geometry. Because of this geometry, IPMSM has a mechanically robust rotor construction, a rotor saliency, and the low effective airgap. These features perimt control of the machine not only in constant torque region but also in constant power region up to a high speed. Higher speed operation over the base speed is required in various applications such as electric vechicle, traction and spindle drives. Such high speed can be achieved with IPMSM by means of flux weakening. Recently some algorithms for flux weakening have been published for IPMSM[3,5,6,7]. A six-step voltage control scheme in constant power region was proposed[5]. This scheme does not have the dependency on the machine parameter for the flux weakening operation. But, in order to change the control mode from constant torque mode into constant power mode, the information of the flux linkage is required. Although this parameter can be compensated according to the variation of the temperature by a thermal sensor, this sensor gives additional cost and reliability penalty to the control system. On the other hand, there was an attempt to utilize the feed-forward torque[6]. But, in this scheme, all the machine parameters are needed to regulate the machine current in the flux weakening region. In [7], a current regulator with feedforward decoupling compensation was proposed for the flux weakening operation. This voltage compensator may well operate in tuned operating conditions. But if there is extra voltage margin due to the weakening of permanent magnet flux linkage according to the temperature rise or DC link voltage variations, the drive system may diverge because of the improper operation of the voltage compensator.

In all previous studies the performance of IPMSM drive system in the extended speed region was strongly dependent on the motor parameters because the model of IPMSM, especially stator voltage equation of the motor, is basically used for the flux weakening control. Unfortunately, the flux linkage of permanent magnet and the stator resistance of the motor are varied according to the temperature[8]. Moreover, the d and q axis self inductance, L_{ds} and L_{qs}, vary with airgap flux[9]. And, the improper tuning of the parameters of IPMSM drive may result in reduced torque capability and stability problems, especially in flux weakening mode.

In this paper, a novel flux weakening control scheme is described. The inverter output voltage, which is the output of the current regulator, is controlled up to the maximum available value related to the dc link voltage by the outer voltage regulating loop. The on-set of flux weakening and the level of the flux are adjusted inherently with the voltage regulating loop. The scheme dose not work on the model of IPMSM for flux weakening control contrast to previous researches, but works on the basis of inverter output voltage regulation. Hence, the scheme has no dependency on the parameters of the IPMSM. Additional feature of the scheme is the guarantee of the performance of the current regulator at any operating condition due to the anti-saturation control of the regulator with the outer voltage feedback loop. The current regulator used in this study is a synchronous PI current regulator with feedforward decoupling loop[6]. Experimental results for a laboratory IPMSM drive system under various operating conditions are presented to verify the feasibility of the proposed control scheme.

II. MODELING OF IPMSM

The machine model for the IPMSM on the d-q synchronous reference frame with an electrical angular velocity ω_e can be represented in the matrix form as followings[1,6,7].

0-7803-3008-0/95 $4.00 © 1995 IEEE

$$\begin{bmatrix} V_{ds}^e \\ V_{qs}^e \end{bmatrix} = \begin{bmatrix} R_s & -\omega_e L_{qs} \\ \omega_e L_{ds} & R_s \end{bmatrix} \begin{bmatrix} i_{ds}^e \\ i_{qs}^e \end{bmatrix} + \begin{bmatrix} 0 \\ \omega_e \psi_f \end{bmatrix} \quad (1)$$

(superscript 'e' denotes the synchronous reference frame)

where, V_{ds}^e, V_{qs}^e : d, q axis components of terminal voltage,

i_{ds}^e, i_{qs}^e : d, q axis components of stator current,

L_{ds}, L_{qs} : d, q axis components of stator self-inductance,

R_s : stator resistance ,

ψ_f :permanent magnet flux linkage.

And the developed torque equation of IPMSM is expressed as follows.

$$T_e = \frac{3}{2} p\left[\psi_f i_{qs}^e + (L_{ds} - L_{qs}) i_{qs}^e i_{ds}^e\right] \quad (2)$$

where, p: the number of pole pairs.

As shown in (2), the electrical torque consists of the magnet alignment torque term produced by flux linkage and the reluctance torque term produced by the saliency ($L_{qs} > L_{ds}$). This feature is the inherent characteristics of this type of machine while only the magnet alignment torque is produced in the other type machine such as surface mount permanent magnet synchronous motor(PMSM). Therefore, it is desirable that the reluctance torque should be properly utilized in order to increase the whole efficiency of the IPMSM drives.

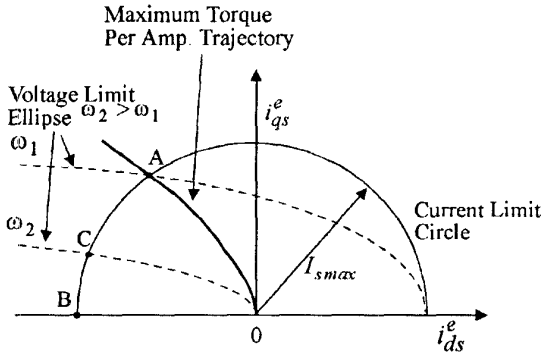

Fig. 1. The maximum torque-per-current trajectory in the $i_{ds}^e - i_{qs}^e$ plane.

In Fig.1, the maximum torque-per-current trajectory on the synchronously rotating d-q current plane is illustrated. When the machine is operated in the constant torque region where from the starting of the machine up to the angular speed, ω_1, in Fig.1, the voltage limit line exceeds the maximum current boundary represented by $I_{s\max}$ which is generally determined by the rating of the machine or the maximum current capability of the power converter. Hence, the voltage limitation is not needed to be considered in this region. The armature current vector might be controlled to fully use the reluctance torque in order to maximize the machine efficiency.

The magnitude of the impressed current vector i_s^e can be expressed as,

$$\left|i_s^e\right| = \sqrt{i_{qs}^{e\,2} + i_{ds}^{e\,2}} \,. \quad (3)$$

From (2) and (3), the d-q axis components of the current vector for the maximum torque-per-ampere are derived as follows:

$$i_{qs}^e = sign(i_s^e) \cdot \sqrt{i_s^{e2} - i_{ds}^{e\,2}} \quad \text{where} \begin{cases} if\ i_s^e \geq 0, & sign(i_s^e) = 1 \\ i_s^e < 0, & sign(i_s^e) = -1 \end{cases} \quad (4)$$

$$i_{ds}^e = \frac{\psi_f - \sqrt{\psi_f^2 + 8(L_{qs} - L_{ds})^2 i_s^{e2}}}{4(L_{qs} - L_{ds})} \quad (5)$$

In the constant torque region, the locus of the current vector according to (4) and (5) is shown as a curve from point 0 to point A in Fig.1.

III. Description of Flux Weakening Control Scheme

A. Operating limits in flux-weakening region

The maximum voltage $V_{s\max}$ that the inverter can supply to the machine is limited by DC link voltage and PWM strategy. In this paper, a PWM strategy based on voltage space vector is used and then $V_{s\max}$ can be identified as $V_{dc}/\sqrt{3}$ [3]. Also the maximum current $I_{s\max}$ is determined by the inverter current rating and machine thermal rating. Therefore the voltage and current of the motor have the following limits [10] :

$$V_{ds}^{e\,2} + V_{qs}^{e\,2} \leq V_{s\max}^{\ 2} \quad (6)$$

$$i_{ds}^{e\,2} + i_{qs}^{e\,2} \leq I_{s\max}^{\ 2} \,. \quad (7)$$

B. Maximum torque operation in flux-weakening region

The torque capability in flux-weakening region is determined by both of the voltage and the current limits. In this region, the currents i_{qs}^e and i_{ds}^e producing the maximum output torque become the values at the crossing point of the current limit circle and voltage limit ellipse[6,7,9]. With the consideration of (6) and (7), The i_{qs}^e and i_{ds}^e for maximum torque operation in flux-weakening region can be modified to followings:

$$i_{qs}^e = sign(i_s^e)\cdot\sqrt{i_s^{e2} - i_{ds}^{e\,2}}$$
$$where \begin{cases} if\ \ i_s^e \geq 0, & sign(i_s^e) = 1 \\ \ \ i_s^e < 0, & sign(i_s^e) = -1 \end{cases} \quad (8)$$

$$i_{ds}^e = \frac{1}{L_{qs}^{\ 2} - L_{ds}^{\ 2}}\Big(L_{ds}\Psi_f - \Big((L_{ds}\Psi_f)^2 + (L_{qs}^{\ 2} - L_{ds}^{\ 2})\Big(\Psi_f^{\ 2} + (L_{ds}i_s^e)^2 - (V_f/\omega_e)^2\Big)\Big)^{\frac{1}{2}}\Big) \quad (9)$$

where, $V_f = V_{s\max} - R_s I_{s\max}$.

In this region, the current vector trajectory should move along the boundary of the current limit circle($A \rightarrow B$) in Fig.1 as rotor speed increases. In other words, the voltage limit ellipse scales inversely with speed so that increasing the speed produces a family of progressively smaller nested ellipses [3].

Without the proper flux weakening at higher speed, the current regulator would be saturated and lose its controllability. Since the onset of current regulator saturation varies according to the load conditions and the machine parameters, the beginning point of flux-weakening and level of the flux should be varied. The late starting of the flux weakening may result in undesired output torque drop, but the early starting deteriorates the acceleration performance. Therefore it is desired to change the onset point of flux weakening according to the load conditions and the machine parameters. From (1) and (7), the optimal point can be deduced as followings.

$$\omega_{base} = \frac{-b + \sqrt{b^2 - 4ac}}{2a} \quad (10)$$

$$\text{where, } \begin{cases} a = (L_{qs}i_{qs}^e)^2 + (L_{ds}i_{ds}^e)^2 + \Psi_f^{\ 2} + L_{ds}\Psi_f i_{ds} \\ b = 2(L_{ds} - L_{qs})R_s i_{ds}^e i_{qs}^e + R_s\Psi_f i_{qs}^e \\ c = R_s^{\ 2}(i_{ds}^{e\ 2} + i_{qs}^{e\ 2}) - V_{s\max}^{\ 2} \end{cases},$$

In high speed region the base speed, ω_{base}, is severely influenced by the permanent magnet flux linkage which varies with operating temperature. And, the q-axis inductance also varies according to the amplitude of q-axis current.

C. Description and Features

Fig. 2 illustrates a block diagram of the speed control system including the proposed flux weakening control algorithm. In Fig. 2 quantities with '*' represent the reference quantities. First, part I is the torque controller in constant torque operating mode. The current command i_s^{e*}, which is the output of the PI speed controller, is decomposed as d and q axis components , i_{dx}^{e*} and i_{qx}^{e*}, according to (4) and (5) along the maximum torque-per-amp trajectory until the current regulator starts to saturate.

Secondly, in the flux-weakening region the controller can be divided to part II and part III. The main idea of the proposed flux weakening control algorithm is the use of the output reference voltage of the synchronous PI current controller to identify the onset of the flux weakening. As the speed of the IPMSM is getting higher during acceleration, the output of the current regulator, especially q axis current regulator, is getting larger and approaches to the boundary of

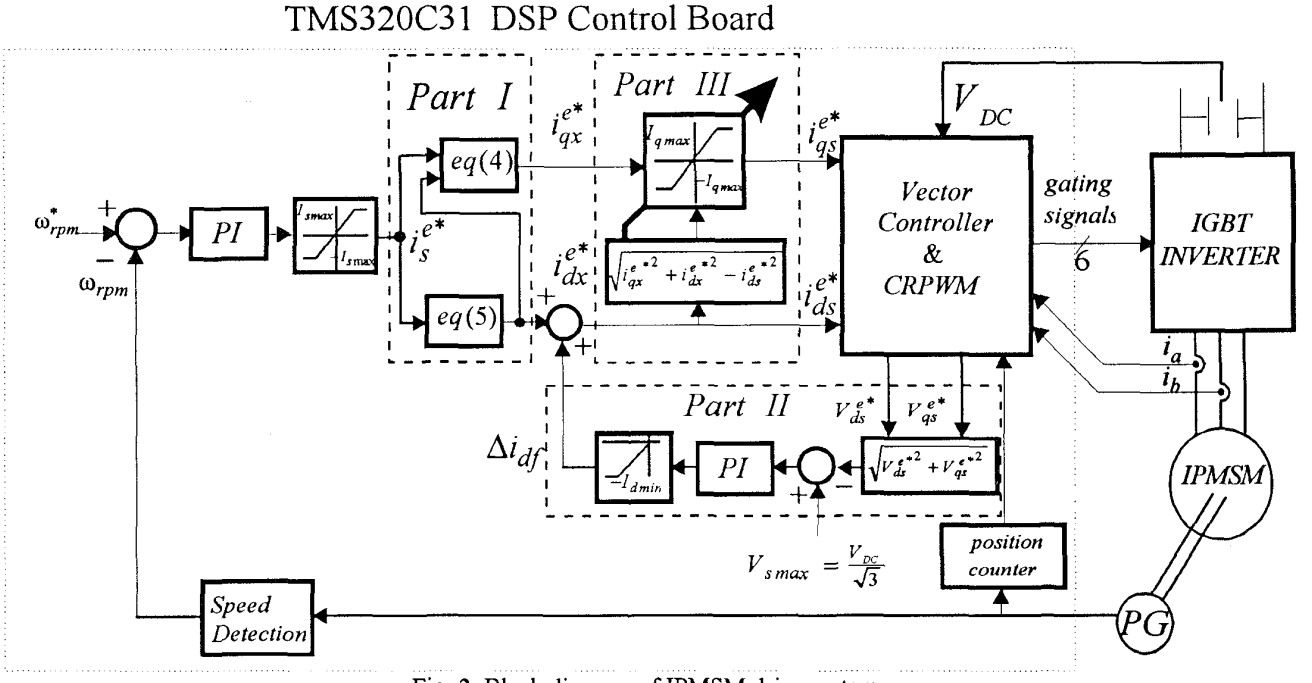

Fig. 2. Block diagram of IPMSM drive system.

the Pulse Width Modulator. Without proper counter measure, the performance of the current regulator is getting worse due to the reduced margin of the voltage and finally it loses its controllability. As shown in Fig.2, the controller in Part II senses the margin of the voltage and increases d axis current toward negative direction to prevent saturation of the current regulator. With thanks to this outer voltage regulating loop the flux level is inherently adjusted and flux weakening is accomplished automatically. At low and intermediate speed region, the magnitude of the output voltage of the current regulator $V_{qds}^{e*}(=\sqrt{V_{ds}^{e*2}+V_{qs}^{e*2}})$ is usually less than $V_{s\max}$ and thus flux-weakening algorithm part II is not activated. Even in this case, if the dc link voltage drops suddenly, the flux weakening operation can be carried out autonomously. The incremental d-axis current Δi_{df}^{e} to control of the flux level of the machine serves as the control input to the d-axis for flux weakening operation, and the limitation of Δi_{df}^{e} is designated as $I_{d\min}=I_{s\max}-I_{d\,rate}$, where $I_{d\,rate}$ is d-axis current at point A in Fig. 1.

The basic action of the control part III is to limit the q-axis current command i_{qx}^{e*} in response to the presence of a growing d-axis current command i_{ds}^{e*} so as to sustain practical ability to regulate the current (i_{ds}^{e}, i_{qs}^{e}) vector along the crossing point of the current limit circle and voltage limit ellipse. The maximum torque-per-ampere under the limitations of the voltage and current is produced at the crossing point of the current limit circle and voltage limit ellipse. And $I_{q\max}$ is determined from i_{qx}^{e*}, i_{ds}^{e*} and Δi_{df}^{e} in part III as shown Fig.2. In constant torque region part III is not activated because i_{ds}^{e*} equals i_{dx}^{e*}, namely Δi_{df}^{e} is zero. By limiting the q-axis current command i_{qx}^{e*} from part III and increasing d-axis current command i_{ds}^{e*} in negative direction from part II at the same time, the current $(i_{ds}^{e*}, i_{qs}^{e*})$ vectors ,which initially lies on the maximum torque-per-ampere locus and inside the voltage limit ellipse at a given speed (the segment : $0 \rightarrow A$), is forced along the boundary of the current limit circle($A \rightarrow B$) in Fig.1 as rotor speed increases. No additional hardware is required to implement the proposed flux weakening algorithm beyond the phase current, the rotor position and speed feedback available for vector rotator and speed control in the already constructed system.

This scheme for flux weakening does not utilized the model of the IMPMSM but the reference output voltage of the synchronous PI current regulator and an outer voltage regulating loop, and thus it is robust and insensitive to the change of the load condition and the machine parameters.

The flux weakening algorithm described above is optimal in the sense of torque generation under the limits of current and voltage at overall operating speed range.

IV. Experimental Results

The system shown in Fig. 2 is implemented with a TMS320C31 DSP Control Board and a Current Regulated PWM IGBT inverter. The switching frequency of the inverter is 5 kHz and space vector PWM algorithm is used for maximum utilization of DC link voltage. The sampling time of current regulation loop is 100 μ sec. and that of outer voltage regulating loop and speed loop is 1 msec. The rotor position and speed for the vector rotator and speed control are obtained with an encoder of 2500 pulse per revolution. The control algorithm including the proposed scheme was fully implemented with the software. The program was written by C-language and size is about 2 k long word.

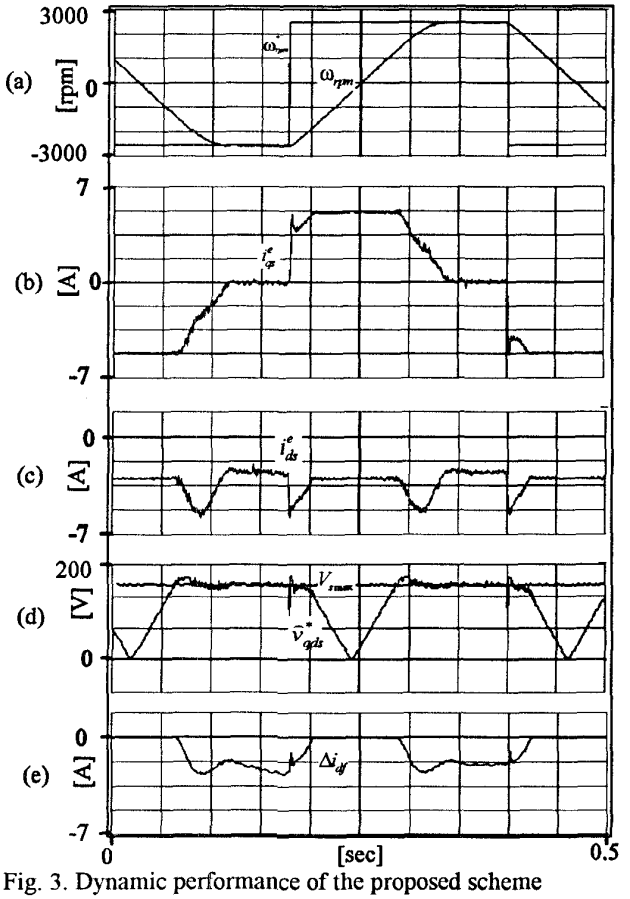

Fig. 3. Dynamic performance of the proposed scheme

When the speed reference changes from -2500 rpm to 2500 rpm and again to -2500 rpm, four-quadrant operation of the drive system, which includes transition between the constant torque and the constant power modes, is shown in Fig. 3. The machine operates well with full performance in

the constant torque region as well as in constant power region in both direction of speed and torque. The transition between the constant torque region and the constant power region is fast and smooth at all conditions of operation. $\hat{V}_{qds}^{e*}$, the trace (d) in Fig.3, is the lowpass filtered output of reference voltage, V_{qds}^{e*}. When $\hat{V}_{qds}^{e*}$ reaches $V_{s\max}$ the flux weakening operation begins at this speed. The error between $V_{s\max}$ and V_{qds}^{e*} feeds the voltage regulating loop. The PI compensator increases d axis current toward negative direction to keep the current regulator from the saturation as shown in Fig.3 (c) and (e). The nominal machine parameters and inverter are shown in Table 1.

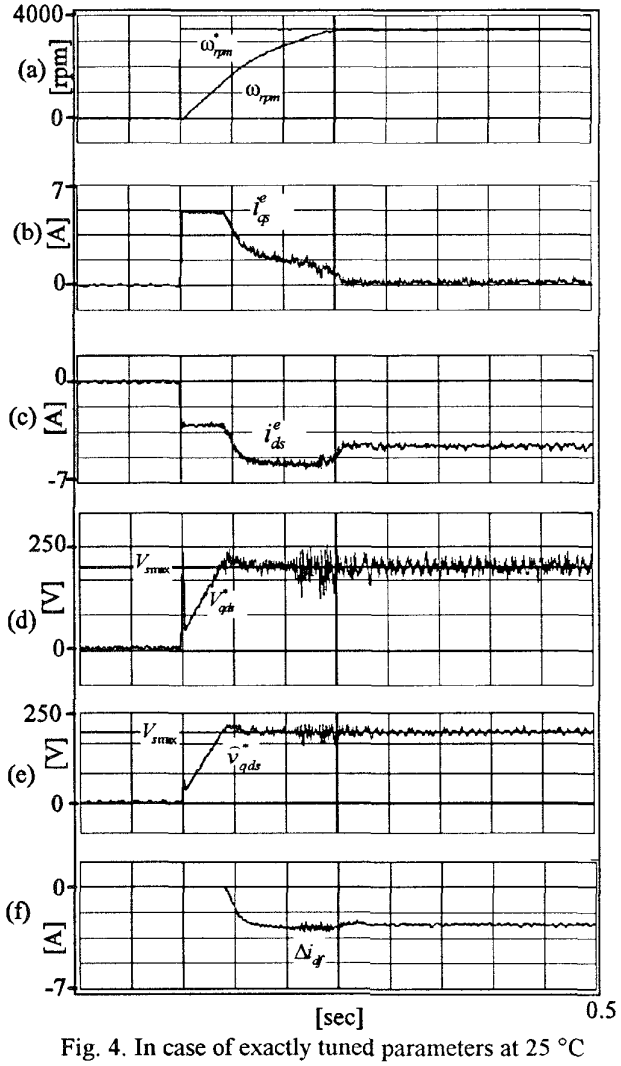

Fig. 4. In case of exactly tuned parameters at 25 °C

The value of $V_{s\max}$ is set according to the dc link voltage. The nominal value of $V_{s\max}$ is about 150 V instead of ideal value 173 V at nominal dc link voltage, 300 V. The voltage difference can be explained as dead time effect, voltage drop of switching device, and the margin of the voltage for current forcing. The unfiltered waveform of V_{qds}^{e*} is shown in Fig. 4 (d), which is very sharp and fluctuating.

To show the operation at the extended speed region the speed command changes from 0 rpm to 3500 rpm in Fig. 4. The machine behaves well as expected. 3500rpm is about twice of the base speed. Fig. 5 shows the dynamic operation with the same condition of Fig.4 except the machine parameters. The parameters are detuned from nominal values to the values at 120 °C. The effect of parameter is shown in only constant torque operation. The difference between the exactly tuned and the detuned case are the decrease of q-axis current and the negative increase of d-axis current in constant torque region.

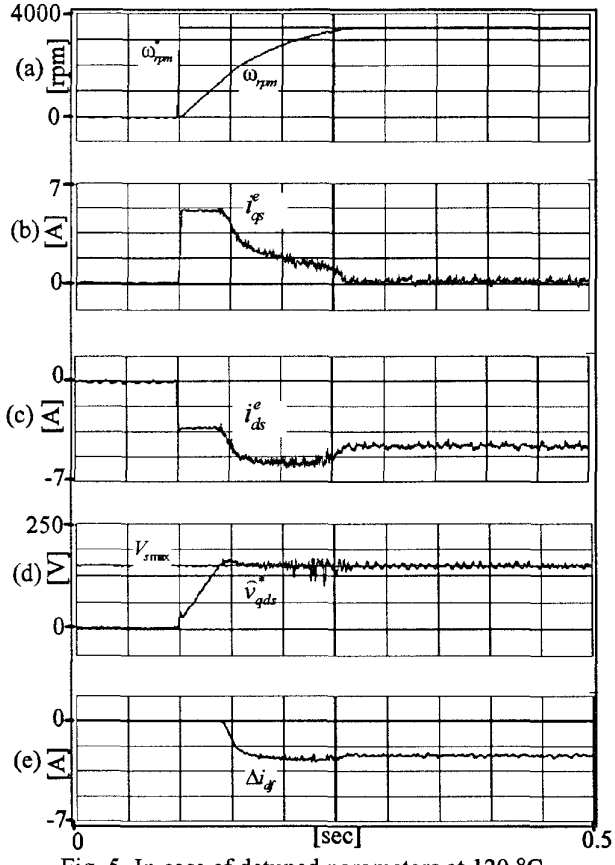

Fig. 5. In case of detuned parameters at 120 °C

By comparing the Fig.4 and Fig.5, the performance of the flux weakening operation is irrespective to the variation of the machine parameters.

V. Conclusions

In this paper, a novel flux weakening control algorithm is proposed. The principal feature of the novel flux weakening

control algorithm is the use of the outer voltage regulating loop. The loop keep the current controller from saturation by adjusting flux level of the machine. And hence the onset of flux weakening and regulation of the flux level is inherently achieved with the feedback of the output reference voltage of the current regulator. Another features of the proposed flux weakening control scheme are no requirement of additional hardware and robustness to the variation of the machine parameters.

The experimental results clarify the effectiveness of the proposed scheme. And it operates well with full performance not only in the constant torque region but also in constant power region in both direction of speed and torque.The transition between the constant torque region and the constant power region is fast and smooth at all operating conditions.

Table 1. Nominal parameters of IPMSM at 25 °C

900[W], 220[V], 4[pole], 1700[rpm]
Rs : 4.3[Ω], Ψ_f : 0.272[Wb], L_{ds} : 27[mH]
L_{qs} : 67[mH], V_{DC}=300[V],
I_{rate}= 3[A], $I_{s\max} = 2I_{rate}$,
J=0.000179[$Kg\,m^2$] (motor and load inertia)

REFERENCES

[1] T. M. Jahns, G. B. Kliman and T. W. Neumann, "Interior Permanent-Magnet Synchronous Motors for Adjustable-Speed Drive," *IEEE Trans. Ind. Appl.*, vol. IA-22, no.4, July/Aug., pp.738~747, 1986.

[2] T. M. Rowan and R. J. Kerkman, "A New Synchronous Current Regulator and an Analysis of Current-Regulated PWM Inverters," *IEEE Trans. Ind. Appl.*, vol. IA-22, no.4, July/Aug., pp.678~690, 1986.

[3] T. M. Jahns, "Flux-weakening Regime Operation of an Interior Permanent-magnet Synchronous Motor Drive," *IEEE Trans. Ind. Appl.*, vol. IA-23, no.4, July/Aug., pp.681~689, 1986.

[4] H. W. Van Der Broeck, et al., "Analysis and Realization of a Pulse-Width Modulator Based on Voltage Space Vectors," *IEEE Trans. Ind. Appl.*, vol. IA-24, no.1, Jan./Feb., pp.142~150, 1988.

[5] B. K. Bose, "A High-Performance Inverter-Fed Drive System of an Interior Permanent Magnet Synchronous Machine", *IEEE Trans. Ind. Appl.*, vol. IA-24, no.6, Sep./Oct., pp.987~997, 1988.

[6] S. R. MacMinn and T. M. Jahns, "Control Techniques for Improved High-Speed Performance of Interior PM Synchronous motor Drives," *IEEE Trans. Ind. Appl.*, vol. IA-27, no. 4, Sep./Oct., pp.997~1004, 1991.

[7] S. Morimoto, M. Sanada and Y. Taketa, "Wide-Speed Operation of Interior Permanent Magnet Synchronous Motors with High-Performance Current Regulator," *IEEE Trans. Ind. Appl.*, vol. IA-30, no.4, July/Aug., pp.920~926, 1994.

[8] T. Sebastian, "Temperature Effects on Torque Production and Efficiency of PM Motors using NdFeB Magnets," in Proc. IEEE/IAS Conf. Rec., pp.78~83, 1993.

[9] B. Sneyers, D. W. Novotny, and T. A. Lipo, "Field weakening in buried permanent magnet ac motor drives," *IEEE Trans. Ind. Appl.*, vol. IA-21, no. 2, Mar./Apr., pp.398~407, 1991.

[10] Sang-Hoon Kim and Seung-Ki Sul, "Voltage Control Strategy for Maximum Torque Operation of Induction Machine in the Field Weakening Region," in Proc. of IECON'94, pp599~604, 1994.